Supporting Information for

A Mass Budget for Mercury and Methylmercury in the Arctic Ocean

Anne L. Soerensen[a,b,c*], Daniel J. Jacob[b], Amina T. Schartup[a,b], Jenny A. Fisher[d], Igor Lehnherr[e,f], Vincent L. St Louis[e], Lars-Eric Heimbürger[g,h,i], Jeroen E. Sonke[g], David P. Krabbenhoft[j], Elsie M. Sunderland[a,b]

[a] Harvard T.H. Chan School of Public Health, Department of Environmental Health, Boston MA 02215, USA

[b] Harvard University, John A. Paulson School of Engineering and Applied Sciences Cambridge MA, 02138, USA

[c] Stockholm University, Department of Environmental Science and Analytical Chemistry, Stockholm, 11418 Sweden

[d] University of Wollongong, Centre for Atmospheric Chemistry, Wollongong NSW, 2522, Australia

[e] University of Alberta, Department of Biological Sciences, Edmonton, Alberta, Canada T6G 2E9

[f] University of Toronto-Mississauga, Department of Geography, Mississauga, Ontario, Canada L5L 1C6

[g] CNRS, Geoscience Environment Toulouse, Midi-Pyrenees Observatory, Toulouse, 31400, France

[h] University of Bremen, Department of Geosciences, Bremen, 28334, Germany

[i] Aix Marseille Université, CNRS/INSU, Université de Toulon, IRD, Mediterranean Institute of Oceanography (MIO) UM 110, 13288, Marseille, France

[j] U.S. Geological Survey, Middleton, Wisconsin 53562, USA

Contents of this file

Introduction

The Supporting Information contains two texts, nine tables, and four figures.

Rate constants

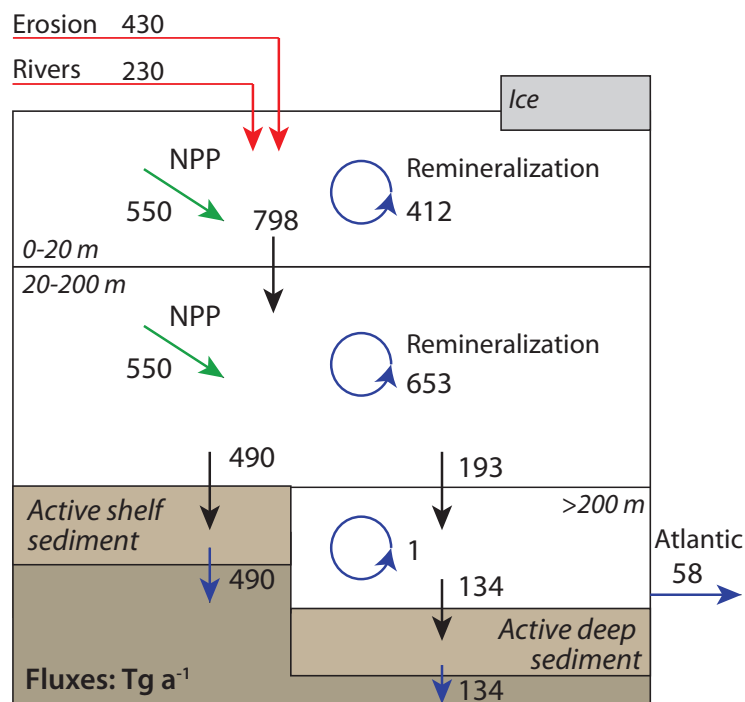**Table S1.** Compilation of measured rate constants for Hg^{II} methylation and MeHg demethylation in seawater.

	avg±stdv (d^{-1})	median (d^{-1})	min-max (d^{-1})	avg±stdv (m^2 E^{-1})	Reference
Methylation					
Unfiltered (dark)	0.0068±0.0039*	0.0050*	0.0006 – 0.013*		[Lehnherr et al., 2011]
Unfiltered (light)	0.0179±0.0197	0.0085	<0.0002 – 0.060		[Monperrus et al., 2007]
Unfiltered (dark)	0.0154±0.0119	0.0130	<0.0002 – 0.038		[Monperrus et al., 2007]
Filtered (light)	0.0072±0.0072	0.0040	<0.0002 – 0.017		[Monperrus et al., 2007]
Filtered (dark)	0.0056±0.0046	0.0060	<0.0002 – 0.013		[Monperrus et al., 2007]
Unfiltered (dark)			<0.0001-0.001		[Sharif et al., 2014]
Unfiltered (light)			<0.0001-0.004		[Sharif et al., 2014]
Filtered (light)			<0.0001-0.003		[Sharif et al., 2014]
Filtered (dark)			<0.0001		[Sharif et al., 2014]
Unfiltered (dark)	0.0025		Max 0.004		[Schartup et al. 2015]
n/a	0.13				[Mason and Sullivan, 1999]
Demethylation					
Unfiltered (dark)	0.36±0.09*		0.23 – 0.59*		[Lehnherr et al., 2011]
Filtered (light)	0.04[a] *			1×10^{-3} *	[Lehnherr et al., 2011]
Filtered (light)	0.2[b] *				[Lehnherr et al., 2011]
n/a			<0.09 – 0.43		[Whalin et al., 2007]
Unfiltered (light)	0.16±0.05	0.159	0.048 – 0.245		[Monperrus et al., 2007]
Unfiltered (dark)	0.06±0.03	0.059	<0.015 – 0.109		[Monperrus et al., 2007]
Filtered (light)	0.09±0.04	0.090	0.033 – 0.139		[Monperrus et al., 2007]
Filtered (dark)	0.05±0.03	0.064	<0.015 – 0.088		[Monperrus et al., 2007]
Unfiltered (light)				3.2(±1.0) ×10^{-3}	[Black et al., 2012]
Unfiltered (light)				9.9(±26.0) ×10^{-3}	[Black et al., 2012]
Unfiltered (dark)			0.07-0.21		[Sharif et al., 2014]
Unfiltered (light)			0.06-0.55		[Sharif et al., 2014]
Filtered (light)			0.08-0.29		[Sharif et al., 2014]
Filtered (dark)			<0.02-0.13		[Sharif et al., 2014]
Dimethylation					
Unfiltered (dark)			nd-0.0016*		[Lehnherr et al., 2011]
Me$_2$Hg decomposition					
Light				<1×10^{-3}	[Black et al., 2009]
n/a			0.0002		[Mason et al., 1995]
Light			0.32 – 1.64		[Mason and Sullivan, 1999]
Dark			0.16 – 0.22		[Mason and Sullivan, 1999]

* Arctic data, [a] 9 days incubation, [b] 24 hours incubation

Budgets

A) Solids budget

Erosion   430

Rivers   230

Ice

NPP
550   798

Remineralization   412

0-20 m

20-200 m

NPP
550

Remineralization   653

490   193   >200 m

Active shelf sediment

490   1   134   Atlantic   58

Active deep sediment

Fluxes: Tg a⁻¹   134

B) Hydrologic budget

Precipitation   Evopotranspiration
3.7   1.3

Rivers 3.3

Ice   2.5

Pacific surface inflow   10.4

Atlantic surface inflow   17.2

Atlantic surface outflow   30.8

0-20 m

20-200 m

Pacific sub-surface inflow   15.6

Atlantic subsurface inflow   110

Atlantic subsurface outflow   107

115   96   Advection   >200 m

Active shelf sediment

Atlantic deep inflow   216

Atlantic deep outflow   235

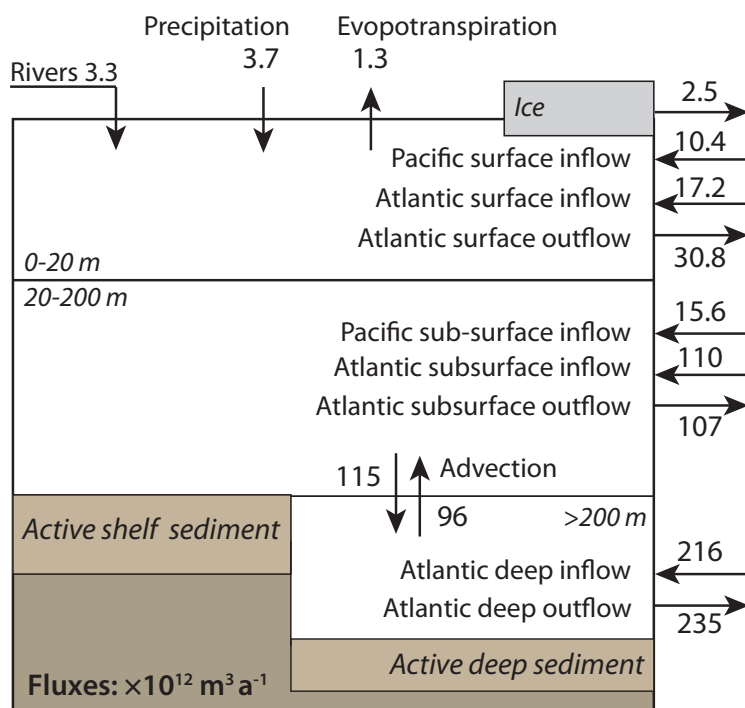Active deep sediment

Fluxes: ×10¹² m³ a⁻¹

Figure S1. A: Solids budget for the Arctic Ocean in Tg a^{-1}. Red arrows denote external sources, green arrows denote internal sources, black arrows denote internal fluxes and blue arrows represent losses. The fraction of solids from rivers and NPP remaining after remineralization at each depth is 50% in the PML, 30% in the subsurface water and 1% in the deep ocean [*Cai et al.*, 2010; *Moran et al.*, 1997; *Rachold et al.*, 2004]. Solids from erosion are assumed not to remineralize. B: Hydrologic budget for external input and losses and internal circulation in the Arctic Ocean (×10^{12} m^3 a^{-1}).
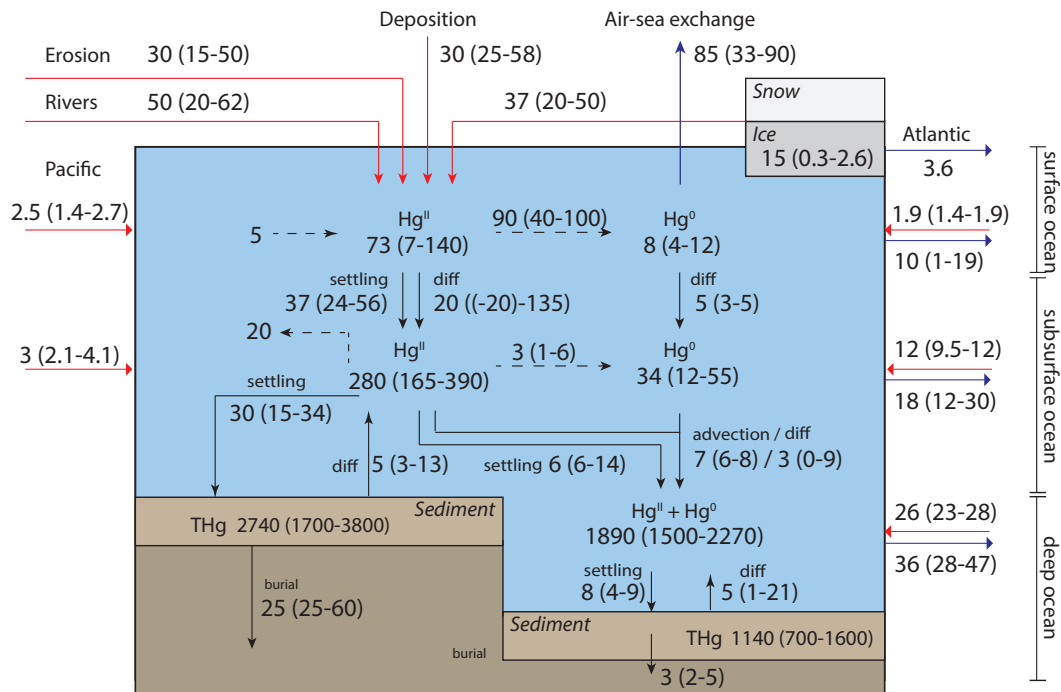
Figure S2. Empirical mass budget for the Arctic Ocean for inorganic Hg species including uncertainty ranges for masses and fluxes not given in Table S2. Red arrows are external sources, black arrows are internal fluxes and blue arrows are losses. Punctuated lines describe net fluxes. Masses are in Mg and fluxes in Mg a^{-1}.
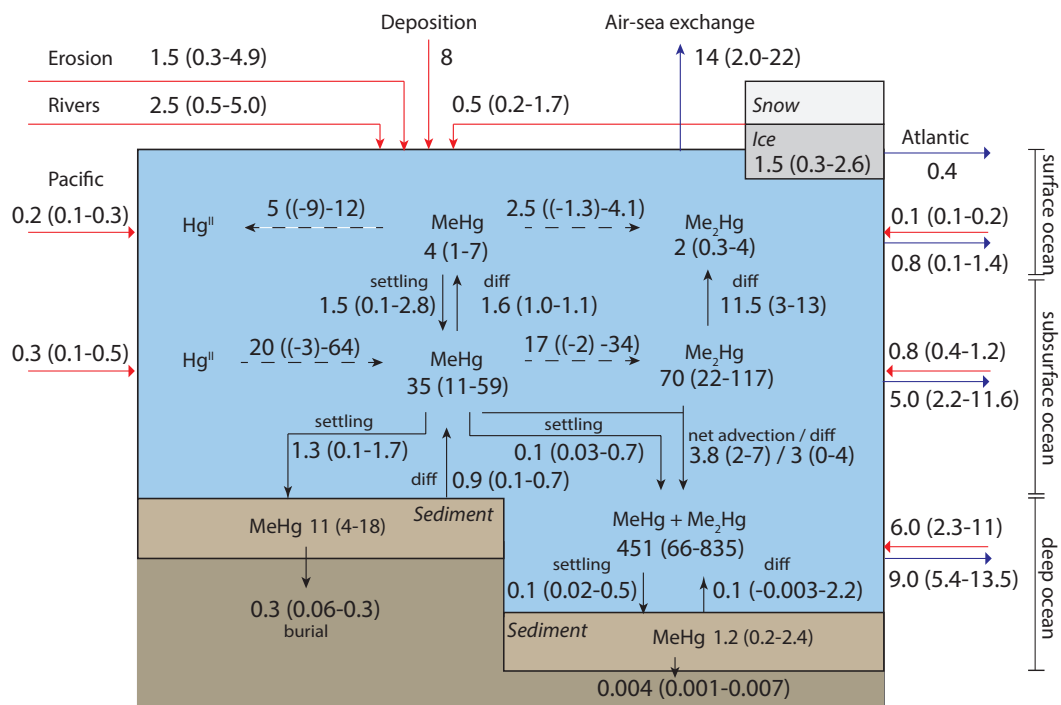

Figure S3. Empirical mass budget for the Arctic Ocean for organic Hg species including uncertainty ranges for masses and fluxes not given in Table S2. Red arrows are external sources, black arrows are internal fluxes and blue arrows are losses. The punctuated lines describe the net flux of biotic methylation/demethylation. Masses are in Mg and fluxes in Mg a^{-1}.

Observations

Text S1. Information on North Atlantic inflow data

Total inorganic Hg and methylated Hg concentrations from the CLIVAR A16N Cruise Track in the North Atlantic for stations occupied in August 2013. Measurements and analytical details were the same as Sunderland et al. (2009). The same depth intervals as in the Arctic were used to calculate average depth concentrations. Data are from station 007 (61.6 N; 20.0 W) and station 015 (58.0 N; 20.0W)(n=24).

0-20 meter, surface: 0.48±0.08 pM Hg,   42±25 fM methylated Hg

20-200 meter, subsurface: 0.50±0.06 pM Hg,   38±18 fM methylated Hg

>200 meter, deep ocean: 0.6±0.06 pM Hg,   153±99 fM methylated Hg

Text S2. Canadian Arctic Archipelago Seawater Samples Collected by I. Lehnherr et al.

Seawater samples were collected at 17 stations across the Canadian Arctic Archipelago (Figure 1), in 2006, 2007 and 2010,between 7-August and 16-October while aboard the *CCGS Amundsen* icebreaker as part of the ArcticNet research program (N = 22, 5 stations were sampled in two separate years). At each station, 12 L Teflon-lined Niskin bottles (General Oceanics) mounted on the ship's rosette system were used to obtain samples from various depths, generally corresponding to the surface (~2-4 m), the subsurface chlorophyll maximum (SCM, the depth of maximum chlorophyll *a* fluorescence and hence algal biomass) and the lower oxycline (a zone of high heterotrophic respiration and organic carbon remineralization) and the bottom of the water column (~5-10 m above the seafloor). Subsamples were collected from the Niskin bottles into pre-cleaned amber Boston round bottles (Environmental Sampling Supplies) using the "clean hands-dirty hands" Hg sampling protocol. All samples were processed and preserved immediately after collection for analysis at a later date. Methylated Hg (MeHg + Me_2Hg) samples were preserved by acidification using trace-metal grade concentrated H_2SO_4 (equivalent to 0.4% of sample volume), the resulting low pH leading to the quantitative conversion of Me_2Hg to MeHg [*Black et al.*, 2009]. Total Hg samples were preserved with the addition of trace-metal grade concentrated HCl (0.2% of sample volume). MeHg samples were preserved by freezing. In 2006, Me_2Hg was collected using the purge and trap technique whereby seawater collected in a custom-made 1 L glass vessel was purged with ultra-high purity (UHP) N_2 gas and the Me_2Hg thus displaced from solution was collected in traps consisting of glass columns packed with Carbo trap. For the 2007 and 2010 data, Me_2Hg was calculated from the difference between methylated Hg and MeHg. Particles (seston) were collected in 2010 by filtering 5-9 L of seawater through 0.2 mm cellulose nitrate membranes. Filter membranes were frozen immediately after sample collection and freeze-dried once back on shore. Sample analysis for methylated Hg, MeHg and total Hg was carried out as described in *Lehnherr et al.* [2011]. MeHg was extracted from particles, by distilling the complete membrane filter, with $Me^{201}Hg$ added as a species-specific internal standard prior to distillation to correct for procedural recoveries, similar to the procedure described for sediments in *Lehnherr et al.* [2012]. The distillate was then analyzed in the same fashion as with seawater samples.

Biota

Table S2. Arctic zooplankton MeHg concentrations

MeHg (ng g^{-1} dw)	MeHg:THg (%)	Reference
Mixed zooplankton		
4±3[A]	70±38	[*Campbell et al.*, 2005]
10±1	28	[*Loseto et al.*, 2008]
95±19	75	[*Loseto et al.*, 2008]
28±0.8[A]	100	[*Campbell et al.*, 2005]
Copepods		
7±1	28	[*Loseto et al.*, 2008]
11±1	34	[*Loseto et al.*, 2008]
7±1	51	[*Pucko et al.*, 2014]
40±9	84	[*Pucko et al.*, 2014]
5-28	10-60	[*Stern and Macdonald*, 2005]
<1.5[A]		[*Jaeger et al.*, 2009]
2±1[A]	8	[*Campbell et al.*, 2005]
Themisto libellula		
66±2	75	[*Loseto et al.*, 2008]
<1.5[A]		[*Jaeger et al.*, 2009]
Themisto abyssorum		
88±10	58	[*Pucko et al.*, 2014]
Chaethognats		
17±4	74	[*Pucko et al.*, 2014]

[A] ng g^{-1} wet weight

Figure S4. Reservoirs of MeHg in plankton and bacteria (note log scale). Note that in the Arctic phytoplankton and zooplankton often has an inverted biomass pyramid and that the zooplankton biomass therefore is higher than that of phytoplankton [*ACIA*, 2005].
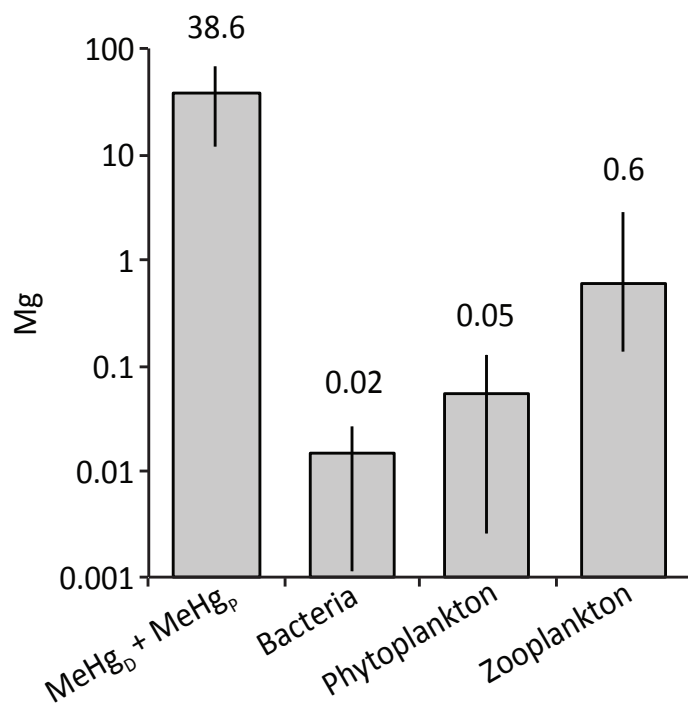
Model parameter description

Table S3. Atmospheric deposition and melt water flux from snow and ice

Deposition			
$M_{dep\text{-}HgII}$ *(Mg a^{-1})*	Hg^{II} deposition to open ocean	30	[*Dastoor and Durnford*, 2014; *Fisher et al.*, 2012]
$M_{dep\text{-}MeHg}$ *(Mg a^{-1})*	MeHg deposition to open ocean based on fast redeposition of evaded Me$_2$Hg	$M_{eva\text{-}Me2Hg} \times F_{open\text{-}ocean\text{-}summer} \times F_{evasion\text{-}summer}$	($F_{open\text{-}ocean\text{-}summer}$; $F_{evasion\text{-}summer}$: Table 3)
Meltwater			
$M_{melt\text{-}HgII}$ *(Mg a^{-1})*	Hg$_{II}$ from meltwater	$C_{melt\text{-}HgII} \times Prec \times (1\text{-}F_{open\text{-}ocean})$	($F_{open\text{-}ocean}$; Prec: Table 3, $C_{melt\text{-}HgII}$: Table 4)
$M_{melt\text{-}MeHg}$ *(Mg a^{-1})*	MeHg from meltwater	$C_{melt\text{-}MeHg} \times Prec \times (1\text{-}F_{open\text{-}ocean})$	($F_{open\text{-}ocean}$; Prec: Table 3, $C_{melt\text{-}MeHg}$: Table 4)
Multi-year sea-ice loss			
$M_{ice\text{-}HgII}$ *(Mg y^{-1})*	Hg^{II} from multi-year sea-ice loss	0.42	[*Beattie et al.*, 2014]
$M_{ice\text{-}MeHg}$ *(Mg y^{-1})*	MeHg from multi-year sea-ice loss	0.042	[*Beattie et al.*, 2014]

Table S4. River and erosion fluxes

$M_{river\text{-}HgII}$ *(Mg a^{-1})*	River Hg^{II} discharge	50	[*Dastoor and Durnford*, 2014; *Zhang et al.*, 2015]
$M_{river\text{-}MeHg}$ *(Mg a^{-1})*	River MeHg discharge	$M_{river\text{-}HgII} \times F_{river\text{-}MeHg}$	
$M_{erosion\text{-}MeHg}$ *(Mg a^{-1})*	Erosion MeHg input	$M_{erosion\text{-}HgII} \times F_{MeHg\text{-}sediment}$	
$M_{erosion\text{-}HgII}$ *(Mg a^{-1})*	Erosion Hg^{II} input	$TSS_{erosion} \times C_{erosion\text{-}HgII} \times 10^{-12}$	
$F_{river\text{-}MeHg}$	MeHg:Hg^{II} fraction in river discharge	0.05 (0.01-0.10)	(Table 4)
$TSS_{erosion}$ *(g a^{-1})*	TSS from erosion	430×10^{12}	(Figure 1)
$C_{erosion\text{-}HgII}$ *(ng g^{-1})*	[Hg^{II}] in eroded TSS	81 (61-114)	[*Leitch*, 2006]
$F_{MeHg\text{-}sediment}$	Fraction of eroded Hg^{II} found as MeHg	0.01	[*Hollweg et al.*, 2010]

Table S5. Chemical transformation in the water column.

M_{ox} (Mg a^{-1})	Oxidation flux	$M_{w-Hg0} \times (k_{phot-ox} + k_{dark-ox}) \times 365$	
M_{red} (Mg a^{-1})	Reduction flux	$M_{w-HgII} \times F_{red} \times (k_{bio-red} + k_{phot-red}) \times 365$	
M_{met} (Mg a^{-1})	Methylation flux	$M_{w-HgII} \times k_{met} \times 365$	
M_{dem} (Mg a^{-1})	Demethylation flux	$M_{w-MeHg} \times (k_{phot-dem} + (k_{bio-dem} \times F_{rad-area})) \times 365$	
M_{met2} (Mg a^{-1})	MeHg to Me$_2$Hg flux	$M_{w-MeHg} \times k_{met2} \times 365$	
M_{2dec} (Mg a^{-1})	Me$_2$Hg decomposition flux	$M_{w-Me2Hg} \times (k_{2dec} + k_{phot-2dec}) \times 365$	
M_w (Mg)	Mass of Hg species in specified reservoir		
$k_{phot-ox}$ (d^{-1})	Photo-oxidation rate constant	$0.57 \times RAD \times (F_{rad-area})$	
$k_{phot-red}$ (d^{-1})	Photo-reduction rate constant	$0.16 \times RAD \times (F_{rad-area})$	
$k_{dark-ox}$ (d^{-1})	Dark oxidation rate constant	0.0086	[*Soerensen et al.*, 2010]
$k_{bio-red}$ (d^{-1})	Biotic reduction rate constant	$0.0450 \times NPP$	[*Soerensen et al.*, 2010] (NPP: Table 3)
k_{met} (d^{-1})	Methylation rate constant	$0.0134 \times NPP + k_{met-base}$	[*Lehnherr et al.*, 2011] (NPP: Table 3)
$k_{met-base}$ (d^{-1})	Methylation base rate	0.0056	[*Monperrus et al.*, 2007]
$k_{phot-dem}$ (m^2 E^{-1} d^{-1})	Photo-demethylation rate constant	$PAR \times 3 \times 10^{-3} \times F_{summer}$	(see Table RATES)
$k_{bio-dem}$ (d^{-1})	Biotic demethylation rate constant	0.07-0.18	
$k_{bio\ dem-base}$ (d^{-1})	Demethylation base rate	0.05	[*Monperrus et al.*, 2007]
k_{met2} (d^{-1})	MeHg to Me$_2$Hg rate constant	0.0016	(see Table RATES)
k_{2dec} (d^{-1})	Me$_2$Hg dark decomposition rate constant	0.0002	(see Table RATES)
$k_{phot-2dec}$ (m^2 E^{-1} d^{-1})	Me$_2$Hg photodecomposition rate constant	$PAR \times 5 \times 10^{-4} \times F_{summer}$	50% of detection limit from *Black et al.* [2009]
F_{red}	Fraction of reducible Hg^{II}	0.4	[*Guentzel et al.*, 1996]
$F_{rad-area}$	Fraction of ocean where light can penetrate during summer (Apr-Sep) months	$F_{open-ocean} + F_{meltp}$	($F_{open-ocean}$: Table 3)
F_{meltp}	Area of ocean with summer melt ponds	0.1	[*Boetius et al.*, 2013]
F_{summer}/ F_{winter}	Fraction of the year considered summer/winter	0.5	
PAR (E m^{-2})	Shortwave intensity as a function of time	$RAD \times 0.432$	
RAD (W m^{-2})	Shortwave intensity at specified depth intervals	$\dfrac{1}{x_2 - x_1} \cdot \dfrac{R_i}{\eta}[e^{\eta x_1} - e^{-\eta x_2}]$	(RAD_i: Table 3)
x_1 (m)	Surface depth		
x_2 (m)	Bottom depth		
η (m^{-1})	Extinction coefficient for radiation	$\eta_w + \eta_{Chl}C_{Chl} + \eta_{DOC}C_{DOC}$	
η_w (m^{-1})	Extinction coefficient for water	450 nm (vis) = 0.0145	
η_{Chla} (m^{-1})	Extinction coefficient for pigments	450 nm (vis) = 31	
C_{Chla} (mg L^{-1})	Average concentration of Chl a in mixed layer	0.6×10^{-3}	[*Galand et al.*, 2008; *Jin et al.*, 2012]
η_{DOC} (mg L^{-1})	Extinction coefficient for DOC	450 nm (vis) = 0.654	
C_{DOC} (mg L^{-1})	Concentration of DOC in water column	0.8	[*Dittmar and Kattner*, 2003; *Hansell et al.*, 2012]

Table S6. Chemical transformation in sediment

$M_{sed\text{-}met}$ (Mg a^{-1})	Sediment methylation flux	$C_{psed\text{-}HgII} \times k_{sed\text{-}met} \times 365$ (d y^{-1})	
$M_{sed\text{-}dem}$ (Mg a^{-1})	Sediment demethylation flux	$C_{psed\text{-}MeHg} \times k_{sed\text{-}dem} \times 365$ (d y^{-1})	
$C_{psed\text{-}HgII}$ (pM)	Porewater Hg^{II} concentration	74.0 (14-258)	$C_{sed\text{-}HgII} \times 10^3 / kd_{HgII}$ (C_{sed}: Table 2)
$C_{psed\text{-}MeHg}$ (pM)	Porewater MeHg concentration	2.4 (0.3-9.9)	$C_{sed\text{-}MeHg} \times 10^3 / kd_{MeHg}$ (C_{sed}: Table 2)
kd_{HgII}	Hg^{II} partition coefficient	$10^{4.0}$ ($10^{3.1}$-$10^{4.2}$)	[*Hollweg et al.*, 2010; *Schartup et al.*, 2015; *Sunderland et al.*, 2010]
kd_{MeHg}	MeHg partition coefficient	$10^{2.7}$ ($10^{2.2}$-$10^{3.1}$)	[*Hollweg et al.*, 2010; *Schartup et al.*, 2015; *Sunderland et al.*, 2010]
$k_{sed\text{-}met}$ (d^{-1})	Sediment methylation rate constant	0.03	[*Hammerschmidt and Fitzgerald, 2008; Heyes et al., 2006; Hollweg et al., 2010*]
$k_{sed\text{-}dem}$ (d^{-1})	Sediment demethylation rate constant	0.58	Derived based on the sediment MeHg:Hg^{II} ratio

Table S7. Sediment burial

M_{burial} (Mg a^{-1})	Burial flux of Hg^{II} and MeHg	$M_{sed} \times Burial / D_{sed}$	Burial rate found in Table 3
M_{sed} (Mg)	Hg species conc. in sediments	$V_{sed} \times Sedsolid \times C_{sed} \times 10^{-15}$ (Mg ng^{-1}) $\times 10^6$ (g kg^{-1} m3 l^{-1}) (C_{sed}: Table 2)	
$Sedsolid$ (kg l^{-1})	Concentration of solids in benthic sediments	$(1-POR) \times DSS$	
DSS (kg l^{-1})	Density of sediment solids	1.5	
V_{sed} (m^3)	Sediment volume	$A_{sed} \times D_{sed}$	(A_{sed}: Table 3)
$D_{sed\text{-}deep}$ (m)	Depth of active deep ocean sediment	0.01	[*Clough et al.*, 1997]
$D_{sed\text{-}shelf}$ (m)	Depth of active shelf sediment	0.02	[*Clough et al.*, 1997; *Kuzyk et al.*, 2013; *Trefry et al.*, 2014]

Table S8. Diffusive transfer

Sediment-water interphase

$M_{sdiff\text{-}HgX}$ (Mg y^{-1})	Sediment-water net diffusion of Hg	$F_{sw\text{-}diff} \times A_{sed} \times 10^4 cm^2\ m^{-2} \times (60 \times 60 \times 24 \times 365\ s\ y^{-1})$	
$F_{sw\text{-}diff}$ (ng cm^{-2} s^{-1})	Diffusive flux based on Fick's law	$\dfrac{POR \times D_{sw}}{TOR} \times \dfrac{(C_{psed\text{-}Hg} - C_{w\text{-}Hg}) \times 1000}{D_{sed}}$	The diffusivity gradient is assumed to be in the top 1 cm of the sediment [*Sunderland et al.*, 2010]
TOR	Tortuosity of sediments	$1 - \ln(POR^2)$	[*Gill et al., 1999*]
POR	Porosity of sediments	0.68 ± 0.10	[Hamden et al., 2013; Kuzyk et al., 2013]
D_{sed} (cm^2 s^{-1})	Sediment-water diffusion coefficient at temperature Tsed	$D_{sw25}\ /\ (1+0.048\times(25-T_{sed}))$	[*Gill et al., 1999*]
D_{sw25} (cm^2 s^{-1})	Sediment-water diffusion coefficient at 25 °C	6×10^{-6} (2×10^{-6}- 12×10^{-6})	[*Hollweg et al.*, 2010]
T_{sed} (°C)	Temperature of sediments	1	Approximation, a 5 °C change in average temperature results in 12-15% change in diffusion flux
A_{sed}	Sediment area		Table 3

Water column diffusion

$M_{wdif\text{-}HgX}$ (Mg y^{-1})	In water column eddy diffusion of X species (Hg^{II}, Hg^0, MeHg, and Me$_2$Hg)	$D_w \times \left(\dfrac{C_{w\text{-}HgX}}{DiffDepth_{z2} - DiffDepth_{z1}}\right) \times 60\times60\times24\times365$	
D_w (m^{2}s^{-1})	Eddy diffusion coefficient	0.8×10^{-4} ($<0.05\times10^{-4}$-2.5×10^{-4})	[*Padman and Dillon*, 1991; *Shaw and Stanton*, 2014; *Wallace et al.*, 1987]
$DiffDepth_{so}$ (m)	Depth of diffusion gradient	20	
$DiffDepth_{ss}$ (m)	Depth of diffusion gradient	140	
$DiffDepth_{de}$ (m)	Depth of diffusion gradient	300	
z1 (m)	Upper diffusion depth		
z2 (m)	Lower diffusion depth		

Table S9. Gas exchange parameterization for Me$_2$Hg

$M_{eva\text{-}Me2Hg}$ (Mg y^{-1})	Total Me$_2$Hg evasion flux (A (areas); F: in Table 3)	$F_v \times \left(A_{shelf} + A_{deep}\right) \times \left(\dfrac{F_{open-sum} + F_{open-win}}{2}\right) \times 10^{-15} \times 24 \times 365$	
F_v (ng m^{-2} h^{-1})	Me$_2$Hg air-sea exchange flux	$K_w(C_w - C_a / H'_X(T))$	
C_a (ng m^{-3})	Concentration of Me$_2$Hg in air	0.0038±0.0031	[*Baya et al.*, 2015]
C_w (ng m^{-3})	Concentrations of Me$_2$Hg in PML		Table 1
$H'_{Me2Hg}(T)$	Temperature dependent dimensionless Henry's law constant for Me$_2$Hg	$\ln H' = (\dfrac{-2512.43}{T} + 7.27)$	[*Lindqvist and Rodhe*, 1985]
K_w (m hr^{-1})	Water-side mass transfer coefficient	$A \times u_{10}^2 (Sc_{HgX} / Sc_{CO_2})^{-0.5}$	[*Wanninkhof*, 1992]
A (unitless)	Constant based on the Weibull distribution of wind speeds over oceans	0.25	[*Nightingale et al.*, 2000]
u_{10} (m s^{-1})	Average wind speed at 10 m above sea surface	5.6 (4-6)	[*Nummelin et al.*, 2015; *Serreze and Barry*, 2005]
Sc_{CO_2}	Schmidt number for CO$_2$	$0.11T'^2 - 6.16T' + 644.7$	[*Poissant et al.*, 2000]
T' (°C)	Water temperature	0	Approximation, a 5 °C change in temperature only lead to 4% change in evasion
TK (K)	Water temperature	T'+273.15	
Sc_{Hg}	Schmidt number for Me$_2$Hg	ν / D	
ν (cm^2 s^{-1})	Kinematic viscosity	$N/\rho = 0.017e^{(-0.025T')}$	[*Poissant et al.*, 2000]
ρ (mg cm^{-3})	Seawater density	1025	
D (cm^2 s^{-1})	Me$_2$Hg diffusivity based on Wilke-Chang	$\dfrac{7.4 \times 10^{-8}(\phi_w M_w)^{1/2} T}{N V_B^{0.6}}$	[*Wilke and Chang*, 1955]
N (cP)	Viscosity of water	See Soerensen et al. (2010)	[*Soerensen et al.*, 2010]
M_w (g mol^{-1})	Molecular weight of water	18.0	
V_B (cm^3 mol^{-1})	Molal volume of Me$_2$Hg at its normal boiling temperature	72.11	
ϕ_w	Solvent association factor	2.26	[*Hayduk and Laudie*, 1974]

References Cited

ACIA (2005), Arctic Climate Impact Assessment (http://www.acia.uaf.edu) Rep., 1042 pp, Cambridge University Press.

Baya, P. A., M. Gosselin, I. Lehnherr, V. L. St Louis, and H. Hintelmann (2015), Determination of Monomethylmercury and Dimethylmercury in the Arctic Marine Boundary Layer, *Environ. Sci. Technol.*, *49*(1), 223-232, doi:10.1021/es502601z.

Beattie, S. A., D. Armstrong, A. Chaulk, J. Comte, M. Gosselin, and F. Y. Wang (2014), Total and Methylated Mercury in Arctic Multiyear Sea Ice, *Environ. Sci. Technol.*, *48*(10), 5575-5582

Black, F. J., C. H. Conaway, and A. R. Flegal (2009), Stability of Dimethyl Mercury in Seawater and Its Conversion to Monomethyl Mercury, *Environ. Sci. Technol.*, *43*(11), 4056-4062

Black, F. J., B. A. Poulin, and A. R. Flegal (2012), Factors controlling the abiotic photo-degradation of monomethylmercury in surface waters, *Geochim. Cosmochim. Acta*, *84*, 492-507

Boetius, A., et al. (2013), Export of Algal Biomass from the Melting Arctic Sea Ice, *Science*, *339*(6126), 1430-1432

Cai, P., M. R. van der Loeff, I. Stimac, E. M. Nothig, K. Lepore, and S. B. Moran (2010), Low export flux of particulate organic carbon in the central Arctic Ocean as revealed by Th-234:U-238 disequilibrium, *J. Geosphys. Res. Oceans*, *115*

Campbell, L. M., R. J. Norstrom, K. A. Hobson, D. C. G. Muir, S. Backus, and A. T. Fisk (2005), Mercury and other trace elements in a pelagic Arctic marine food web (Northwater Polynya, Baffin Bay), *Sci. Total. Environ.*, *351*, 247-263

Clough, L. M., W. G. Ambrose, J. K. Cochran, C. Barnes, P. E. Renaud, and R. C. Aller (1997), Infaunal density, biomass and bioturbation in the sediments of the Arctic Ocean, *Deep-Sea Res., Part li*, *44*(8), 1683-1704

Dastoor, A., and D. Durnford (2014), Arctic Ocean: Is it a sink or a source of atmospheric mercury?, *Environ. Sci. Technol.*, *48*(3), 1707-1717, doi:10.1021/es404473e.

Dittmar, T., and G. Kattner (2003), The biogeochemistry of the river and shelf ecosystem of the Arctic Ocean: a review, *Mar. Chem.*, *83*(3-4), 103-120

Fisher, J. A., D. J. Jacob, A. L. Soerensen, H. M. Amos, A. Steffen, and E. M. Sunderland (2012), Riverine source of Arctic Ocean mercury inferred from atmospheric observations, *Nature Geosci.*, *5*(7), 499-504

Galand, P. E., C. Lovejoy, J. Pouliot, and W. F. Vincent (2008), Heterogeneous archaeal communities in the particle-rich environment of an arctic shelf ecosystem, *J. Mar. Sys.*, *74*(3-4), 774-782, doi:10.1016/j.jmarsys.2007.12.001.

Gill, G. A., N. S. Bloom, S. Cappellino, C. T. Driscoll, C. Dobbs, L. McShea, R. Mason, and J. W. M. Rudd (1999), Sediment-water fluxes of mercury in Lavaca Bay, Texas, *Environ. Sci. Technol.*, *33*(5), 663-669

Guentzel, J. L., R. T. Powell, W. M. Landing, and R. P. Mason (1996), Mercury associated with colloidal material in an estuarine and an open-ocean environment, *Mar. Chem.*, *55*(1-2), 177-188

Hamden, L. J., R. B. Coffin, M. Sikaroodi, J. Greinert, T. Treude, and P. M. Gillevet (2013), Ocean currents shape the microbiome of Arctic marine sediments, *The ISME Journal*, *7*, 685-696

Hammerschmidt, C. R., and W. F. Fitzgerald (2008), Sediment-water exchange of methylmercury determined from shipboard benthic flux chambers, *Mar. Chem.*, *109*(1-2), 86-97

Hansell, D. A., C. A. Carlson, and R. Schlitzer (2012), Net removal of major marine dissolved organic carbon fractions in the subsurface ocean, *Glob. Biogeochem. Cycles*, *26*

Hayduk, W., and H. Laudie (1974), Prediction of diffusion-coefficients for nonelectrolytes in dilute aqueous solutions, *Aiche Journal*, *20*(3), 611-615

Heyes, A., R. P. Mason, E. H. Kim, and E. Sunderland (2006), Mercury methylation in estuaries: Insights from using measuring rates using stable mercury isotopes, *Mar. Chem.*, *102*(1-2), 134-147, doi:10.1016/J.Marchem.2005.09.018.

Hollweg, T. A., C. C. Gilmour, and R. P. Mason (2010), Mercury and methylmercury cycling in sediments of the mid-Atlantic continental shelf and slope, *Limnol. Ocean.*, *55*(6), 2703-2722

Jaeger, I., H. Hop, and G. W. Gabrielsen (2009), Biomagnification of mercury in selected species from an Arctic marine food web in Svalbard, *Sci. Total. Environ.*, *407*(16), 4744-4751

Jin, M. B., C. Deal, S. H. Lee, S. Elliott, E. Hunke, M. Maltrud, and N. Jeffery (2012), Investigation of Arctic sea ice and ocean primary production for the period 1992-2007 using a 3-D global ice-ocean ecosystem model, *Deep-Sea Res., Part li, 81-84*, 28-35

Kuzyk, Z. Z. A., C. Gobeil, and R. W. Macdonald (2013), 210Pb and 137Cs in margin sediments of the Arctic Ocean: Controls on boundary scavenging, *Glob. Biogeochem. Cycles*(27), 1-18, doi:10.1002/gbc.20041.

Lehnherr, I., V. L. St Louis, H. Hintelmann, and J. L. Kirk (2011), Methylation of inorganic mercury in polar marine waters, *Nat. Geosci.*, *4*(5), 298-302

Lehnherr, I., V. L. St. Louis, C. A. Emmerton, J. D. Barker, and J. L. Kirk (2012), Methylmercury cycling in High Arctic wetland ponds: Sources and sinks, *Environ. Sci. Technol.*, *46*(19), 10514-10522

Leitch, D. R. (2006), Mercury distribution in water and permafrost of the lower Mackenzie Basin, their contribution to the mercury contamination in the Beaufort Sea marine ecosystem, and potential effects of climate variation, 130 pp, University of Manitoba, Winnipeg, Manitoba.

Lindqvist, O., and H. Rodhe (1985), Atmospheric Mercury - a Review, *Tellus Series B-Chemical and Physical Meteorology*, *37*(3), 136-159

Loseto, L. L., G. A. Stern, D. Deibel, T. L. Connelly, A. Prokopowicz, D. R. S. Lean, L. Fortier, and S. H. Ferguson (2008), Linking mercury exposure to habitat and feeding behaviour in Beaufort Sea beluga whales, *J. Mar. Sys.*, *74*(3-4), 1012-1024

Mason, R. P., and K. A. Sullivan (1999), The distribution and speciation of mercury in the South and equatorial Atlantic, *Deep-Sea Res., Part li*, *46*(5), 937-956

Mason, R. P., K. R. Rolfhus, and W. F. Fitzgerald (1995), Methylated and Elemental Mercury Cycling in Surface and Deep-Ocean Waters of the North-Atlantic, *Water, Air, Soil Pollut.*, *80*(1-4), 665-677

Monperrus, M., E. Tessier, D. Amouroux, A. Leynaert, P. Huonnic, and O. F. X. Donard (2007), Mercury methylation, demethylation and reduction rates in coastal and marine surface waters of the Mediterranean Sea, *Mar. Chem.*, *107*(1), 49-63

Moran, S. B., K. M. Ellis, and J. N. Smith (1997), Th-234/U-238 disequilibrium in the central Arctic Ocean: implications for particulate organic carbon export, *Deep-Sea Res., Part li*, *44*(8), 1593-1606

Nightingale, P., G. Malin, C. Law, W. AJ, P. Liss, M. Liddicoat, J. Boutin, and R. Upstill-Goddard (2000), In situ evaluation of air-sea gas exchange parameterizations using novel conservative and volatile tracers, *Glob. Biogeochem, Cycles*, *14*(1), 373-387

Nummelin, A., C. Li, and L. H. Smedsrud (2015), Response of Arctic Ocean stratification to changing runoff in a column model, *J. Geophys. Res.: Oceans*, *120*, doi:10.1002/2014JC010571.

Padman, L., and T. M. Dillon (1991), Turbulent mixing near the Yermak Plateau during the coordinated Eastern Arctic Experiment, *J. Geophys. Res.: Oceans (1978–2012)*, *96*(C3), 4769-4782

Poissant, L., M. Amyot, M. Pilote, and D. Lean (2000), Mercury water-air exchange over the upper St. Lawrence River and Lake Ontario, *Environ. Sci. Technol.*, *2000*(34), 3069-3078

Pucko, M., A. Burt, W. Walkusz, F. Wang, R. W. Macdonald, S. Rysgaard, D. G. Barber, J. E. Tremblay, and G. A. Stern (2014), Transformation of Mercury at the Bottom of the Arctic Food Web: An Overlooked Puzzle in the Mercury Exposure Narrative, *Environ. Sci. Technol.*, *48*(13), 7280-7288, doi:10.1021/es404851b.

Rachold, V., H. Eicken, V. V. Gordeev, H. Grigoriev, H.-W. Hubberten, A. P. Lisitzin, L. Shevchenko, and L. Schirmeister (2004), Modern Terrigeneous Organic Carbon Input to the Arctic Ocean, in *The Organic Carbon Cycle in the Arctic Ocean*, edited by R. Stein and R. W. Macdonald, pp. 33-55, Springer, Berlin Heidelberg.

Schartup, A. T., P. H. Balcom, A. L. Soerensen, K. J. Gosnell, R. S. D. Calder, R. P. Mason, and E. M. Sunderland (2015), Freshwater discharges drive high levels of methylmercury in Arctic marine biota, *PNAS*, *112*(38), 11789-11794, doi:10.1073/pnas.1505541112.

Serreze, M. C., and R. G. Barry (2005), *The Arctic Climate System*, Cambridge University Press, United Kingdom.

Sharif, A., M. Monperrus, E. Tessier, S. Bouchet, H. Pinaly, P. Rodriguez-Gonzales, P. Maron, and D. Amouroux (2014), Fate of mercury species in the coastal plume of the Adour River estuary (Bay of Biscay, SW France), *Sci. Total. Environ.*, *496*, 701-713, doi:http://dx.doi.org/10.1016/j.scitotenv.2014.06.116.

Shaw, W. J., and T. P. Stanton (2014), Vertical diffusivity of the Western Arctic Ocean halocline, *Journal of Geophysical Research: Oceans*, *119*(8), 5017-5038

Soerensen, A. L., E. M. Sunderland, C. D. Holmes, D. J. Jacob, R. M. Yantosca, H. Skov, J. H. Christensen, S. A. Strode, and R. P. Mason (2010), An Improved Global Model for Air-Sea Exchange of Mercury: High Concentrations over the North Atlantic, *Environ. Sci. Technol.*, *44*(22), 8574-8580, doi:10.1021/Es102032g.

Stern, G. A., and R. W. Macdonald (2005), Biogeographic provinces of total and methyl mercury in zooplankton and fish from the Beaufort and Chukchi seas: Results from the SHEBA drift, *Environ. Sci. Technol.*, *39*(13), 4707-4713

Sunderland, E. M., J. Dalziel, A. Heyes, B. A. Branfireun, D. P. Krabbenhoft, and F. A. P. C. Gobas (2010), Response of a Macrotidal Estuary to Changes in Anthropogenic Mercury Loading between 1850 and 2000, *Environ. Sci. Technol.*, *44*(5), 1698-1704, doi:10.1021/Es9032524.

Trefry, J. H., R. P. Trocine, L. W. Cooper, and K. H. Dunton (2014), Trace metlas and organic carbon in sediments of the northeastern Chukchi Sea, *Deep-Sea Res., Part li*, *In press*, doi:10.1016/j.dsr2.2013.07.018.

Wallace, D. W., R. M. Moore, and E. P. Jones (1987), Ventilation of the Arctic Ocean cold halocline: rates of diapycnal and isopycnal transport, oxygen utilization and primary production inferred using chlorofluoromethane distributions, *Deep Sea Research Part A. Oceanographic Research Papers*, *34*(12), 1957-1979

Wanninkhof, R. (1992), Relationship between Wind-Speed and Gas-Exchange over the Ocean, *J. Geosphys. Res. Oceans*, *97*(C5), 7373-7382

Whalin, L., E. H. Kim, and R. Mason (2007), Factors influencing the oxidation, reduction, methylation and demethylation of mercury species in coastal waters, *Mar. Chem.*, *107*(3), 278-294, doi:10.1016/j.marchem.2007.04.002.

Wilke, C. R., and P. Chang (1955), Correlation of Diffusion Coefficients in Dilute Solutions, *AIChE J.*, *1*(2), 264-270

Zhang, Y., D. J. Jacob, S. Dutkiewicz, H. M. Amos, and C. J. Sunderland (2015), Biogeochemical drivers of the fate of riverine mercury disharged to the global and Arctic oceans, *Glob. Biogeochem. Cycles*, *29*, doi:10.1002/2015GB005124.